Recoil in vacuum for Te ions: Calibration, models, and applications to radioactive-beam *g*-factor measurements

A. E. Stuchbery
Department of Nuclear Physics, Australian National University, Canberra ACT 0200, Australia

N. J. Stone
Department of Physics, University of Oxford, Oxford OX1 3PU, United Kingdom and Department of Physics and Astronomy, University of Tennessee, Knoxville, Tennessee 37996, USA

(Received 12 February 2007; published 6 September 2007)

In the light of new g factor results for the stable isotopes between ^{122}Te and ^{130}Te, the calibration and modeling of the recoil-in-vacuum (RIV) interaction for Te ions is reexamined, and the recent radioactive-beam g factor measurement on ^{132}Te by the RIV technique is reevaluated. The implications for further RIV g-factor measurements in the ^{132}Sn region are discussed.

DOI: 10.1103/PhysRevC.76.034307 PACS number(s): 21.10.Ky, 25.70.De, 27.60.+j, 23.20.Nx

I. INTRODUCTION

Precise g factor measurements on the stable Te isotopes have been reported in an accompanying paper [1]. The present communication concerns the implications of those data for the calibration and application of the recoil in vacuum (RIV) technique to measure the g factors of excited states in nuclei near ^{132}Sn produced as radioactive beams. For the most part the focus here will be on the pioneering radioactive beam measurement of Stone *et al*. [2] in which the g factor of the first-excited state of ^{132}Te was measured by the RIV technique. Attention will also be given to the calibration requirements for future RIV measurements on ^{134}Te and ^{136}Te, which have 2_1^+-state lifetimes that are considerably shorter and longer, respectively, than those used to date to calibrate the RIV interaction for Te ions.

The paper is arranged as follows. After a review of the theoretical formalism and previous work on RIV in Sec. II, an essentially empirical approach is used to calibrate and reevaluate $g(2_1^+)$ in ^{132}Te (Sec. III). Although this procedure is based on sound conclusions from previous studies, it remains empirical in that no theoretical constraints are placed on the RIV model parameters. Section IV therefore considers more specific models of the RIV interaction that seek to describe the behavior of the free-ion hyperfine fields for Te ions in terms of a few physically meaningful parameters. The extent to which the procedure used to extract the g factor in ^{132}Te is justified is examined in Sec. V. This section includes a discussion of the implications for the calibration of future RIV g-factor measurements on ^{134}Te and ^{136}Te. A summary and concluding remarks follow (Sec. VI).

II. RIV—A SHORT REVIEW

When a free ion moves through vacuum, the hyperfine interaction couples the atomic spin $\boldsymbol{J}$ to the nuclear spin $\boldsymbol{I}$ and together they precess about the total spin $\boldsymbol{F} = \boldsymbol{I} + \boldsymbol{J}$, as illustrated in Fig. 1 (left panel). The precession frequency $\omega_{FF'}$ is proportional to the nuclear g factor and the magnitude of the hyperfine magnetic field at the nucleus. To measure the g factor in ^{132}Te, the 2_1^+ state was Coulomb excited on a ^{12}C target and then allowed to recoil into vacuum. The effect of the hyperfine interaction was observed via the perturbation of the angular correlation of the γ-rays deexciting the 2^+ state [2].

Recoil-in-vacuum (RIV) can refer to two quite distinct experimental techniques, depending on whether the ion has a very simple, few-electron configuration, or whether it has a complex many-electron configuration [3–5]. A version of the RIV technique to measure the first-excited state g factors of H-like light ions ($Z < 20$) produced by fast fragmentation is under development [6]. The focus here is on the application of the RIV technique to slower-moving many-electron radioactive ions [2].

In the presence of vacuum deorientation, the particle-γ angular correlation after Coulomb excitation takes the form (see Refs. [7,8] and references therein)

$$W(\theta_p, \theta_\gamma, \Delta\phi) = \sum_{kq} B_{kq}(\theta_p) Q_k G_k F_k D^{k*}_{q0}(\Delta\phi, \theta_\gamma, 0), \qquad (1)$$

where the angles are defined in Fig. 1 and $\Delta\phi = \phi_p - \phi_\gamma$. The attenuation coefficients, G_k, specify the vacuum deorientation effect; $B_{kq}(\theta_p)$ is the statistical tensor, which defines the spin alignment of the initial state. F_k represents the usual F-coefficient for the γ-ray transition, Q_k is the attenuation factor for the finite size of the γ-ray detector, and $D^{k*}_{q0}(\Delta\phi, \theta_\gamma, 0)$ is the rotation matrix. In the applications of interest $k = 0, 2, 4$. The coordinate frame is right-handed with the beam along the positive z-axis.

The time-dependent attenuation coefficient for an electronic configuration of spin J, which produces a magnetic field B at the nucleus, is given by

$$G_k(t) = \sum_{F,F'} C^{FF'}_{IJ}(k) \cos(\omega_{FF'} t), \qquad (2)$$

where

$$C^{FF'}_{IJ}(k) = \frac{(2F+1)(2F'+1)}{2J+1} \begin{Bmatrix} F & F' & k \\ I & I & J \end{Bmatrix}^2 \qquad (3)$$

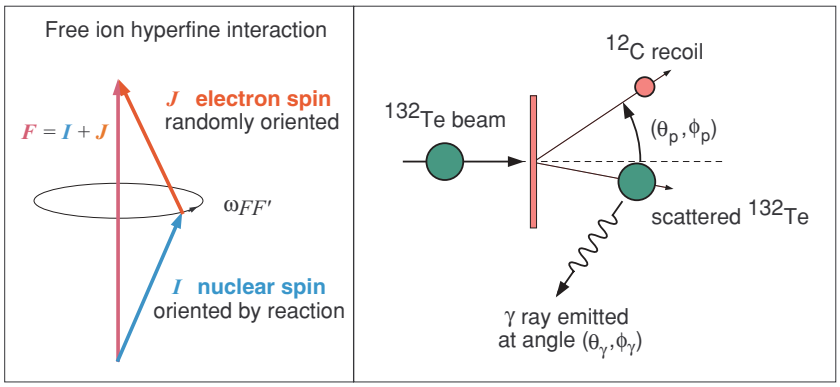

FIG. 1. (Color online) Left: The free-ion hyperfine interaction on which the recoil in vacuum technique is based. Right: Reaction kinematics for the ^{132}Te g-factor measurement.

and

$$\omega_{FF'} = g\frac{\mu_N}{\hbar}B\frac{(F(F+1)-F'(F'+1))}{2J}. \quad (4)$$

The experiments considered here determine the time-integral attenuation factors

$$G_k(\infty) = \int_0^\infty G_k(t)e^{-t/\tau}dt/\tau, \quad (5)$$

where τ is the mean life of the nuclear state.

For an ensemble of many-electron ions with a wide distribution of electron configurations the attenuation coefficient is given by

$$G_k = \sum_i w_i G_k^i, \quad (6)$$

where G_k^i is the deorientation coefficient for ions in the state i and w_i is the fraction of ions in that state. The weights are normalized so that $\sum w_i = 1$.

A superposition of many hyperfine frequencies gives a quasiexponential time dependence to the vacuum attenuation factors, $G_k(t)$. Thus the alignment of the nuclear state, and hence the anisotropy of the γ-ray angular correlation, decreases approximately exponentially with time, at a rate that depends on the magnitude of the nuclear g factor.

In early work the near exponential time dependence of experimental vacuum attenuation coefficients was often interpreted in terms of the Abragam-Pound theory [9] and taken as evidence that the interaction is predominantly fluctuating in character [10–12]. More recent investigations have demonstrated convincingly that the RIV interaction is predominantly a static interaction, due to the superposition of a large number of hyperfine frequencies [13,14]. Although a Gaussian distribution of frequencies is better justified from a physical point of view, the use of a Lorentzian distribution centered at $B = 0$ leads to simpler mathematics and an analytical result [15,16]:

$$G_k(t) = \frac{2}{\pi}\int_0^\infty \sum_{F,F'} C_{IJ}^{FF'}(k)\cos(\omega_{FF'}t)\frac{\Gamma}{\Gamma^2+\omega^2}d\omega \quad (7)$$

$$= \sum_{F,F'} C_{IJ}^{FF'}(k)e^{-|\Gamma_J^{FF'}|t}, \quad (8)$$

where the parameters of the Lorentzian distribution are $\omega = g\mu_N B/\hbar$ and $\Gamma = g\mu_N\Gamma_B/\hbar$; Γ_B is the width at half-maximum of the magnetic field distribution, and $\Gamma_J^{FF'} = \Gamma[F(F+1) - F'(F'+1)]/2J$. The time-integrated attenuation coefficient is given by

$$G_k(\infty) = \sum_{F,F'} C_{IJ}^{FF'}(k)\frac{1}{1+|\Gamma_J^{FF'}|\tau}. \quad (9)$$

Numerical calculations show that the result of the sum is such that, to an excellent approximation,

$$G_k(\infty) = \alpha_k + (1-\alpha_k)\frac{1}{1+|\Gamma_k|\tau}, \quad (10)$$

where Γ_k is directly proportional to $|g|$. In fact most previous workers have absorbed the sum over spins into the Lorentzian frequency distribution, in which case Eq. (10) is exact within the assumptions of their model [15,16]. In general, the relationship between Γ_2, Γ_4, α_2 and α_4 depends on both I and J. For many-electron ions the interaction is so complex that quantitative calculations from first principles are not possible at present. Thus α_k and Γ_k must be treated as parameters. A calibration using isotopes with known g factors and level lifetimes is essential. Measurements on stable beams of ^{122}Te, ^{126}Te, and ^{130}Te with energies of 3 MeV/nucleon were used to calibrate the ^{132}Te radioactive beam measurement [2].

III. REEVALUATION OF $g(2_1^+)$ IN ^{132}Te

Table I summarizes the relevant information needed to evaluate $g(2_1^+)$ in ^{132}Te. Further details of the experiment have been reported in Refs. [2,17–19]. The G_k values here differ slightly from those reported previously [2] because (i) the analysis program has been upgraded to perform the integration

TABLE I. First-excited state g factors, lifetimes and time-integrated vacuum attenuation coefficients.

Isotope	g[a]	τ[b] (ps)	G_2[c]	G_4[c]
^{122}Te	+0.353(14)	10.76(10)	0.358(19)	0.217(11)
^{126}Te	+0.339(13)	6.52(14)	0.506(20)	0.370(12)
^{130}Te	+0.351(18)	3.31(8)	0.628(19)	0.506(13)
^{132}Te		2.6(2)	0.701(26)	0.532(17)

[a] Adopted average values from [1].
[b] Lifetimes from [20–22].
[c] See [2] and text.

over the energy loss of the beam in the target, and (ii) the calculated statistical tensors now include a small contribution due to feeding from higher-excited states.

An empirical extrapolation of the calibration data, based mainly on the Lorentzian static model outlined above, will be used here to reevaluate $g(2_1^+)$ in ^{132}Te. The validity of this approach will then be examined by comparing the data with alternative and more realistic models of the RIV interaction (Sec. IV).

To extract the g factor, the attenuation factors, $G_k(t)$, were assumed to have an exponential time dependence giving time-integral coefficients of the form in Eq. (10). For a more general examination of the data the decay constant was put proportional to $|g^n|$, such that $n = 1$ corresponds to the static limit whereas $n = 2$ corresponds to the fluctuating limit [9]. Thus

$$G_k(t) = \alpha_k + (1 - \alpha_k)e^{-\Gamma_k t}, \tag{11}$$

where

$$\Gamma_k = |g^n|/C_k, \tag{12}$$

and C_k is the parameter that determines the strength of the deorientation.

A number of fits to the G_k values for the stable Te isotopes were performed to explore the parameter space. It was found that the best fit always had $\alpha_2 = \alpha_4 = 0$. These 'hard core' parameters were therefore set to zero for subsequent fits. Acceptable fits could be obtained with $n = 1$, which corresponds to the static limit, or $n = 2$, the fluctuating limit. However the case of $n = 2$ can be excluded as being unphysical (see below and [4,13,14,23]). Thus to fit the data in Table I it is sufficient to take

$$G_k(\infty) = C_k/(C_k + |g|\tau). \tag{13}$$

The empirical form assumed for the attenuation coefficients is therefore that of a static model with a Lorentzian frequency distribution, as in Eq. (10), but with negligible hard core terms.

A simultaneous fit to the G_k values for ^{122,126,130,132}Te, with C_2, C_4 and $g(^{132}\text{Te})$ as parameters, is shown in Fig. 2. The best fit has a chi-squared per degree of freedom, $\chi_\nu^2 = 1.19$, for $\nu = 5$ degrees of freedom, $C_2 = 2.14 \pm 0.11$ ps and $C_4 = 1.18 \pm 0.05$ ps. The resultant g factor for ^{132}Te is $g = (+)0.382^{+0.035}_{-0.033}$,

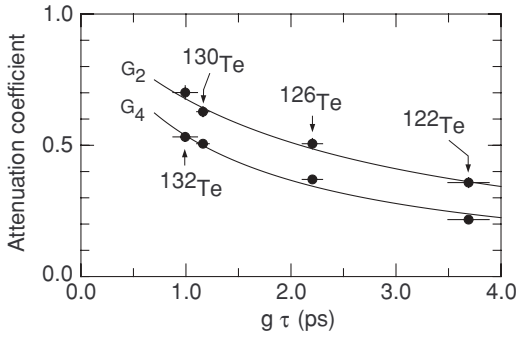

FIG. 2. Time-integral attenuation coefficients for the Te isotopes. The solid line is the best fit to Eq. (13) from which $g(2^+)$ in ^{132}Te was determined.

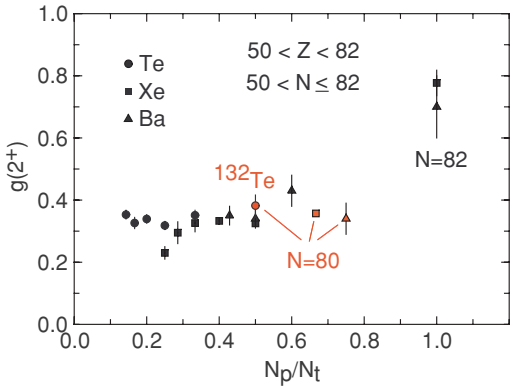

FIG. 3. (Color online) $g(2_1^+)$ systematics in the $A \sim 130$ region. Experimental g factors (see [24–26] and references therein) are plotted versus the valence proton fraction, N_p/N_t, which is defined as in the interacting boson model [27].

where the sign is from systematics. Symmetrizing the error bar and increasing it by $\sqrt{\chi_\nu^2}$, gives $g = (+)0.382 \pm 0.037$, which may be rounded to give

$$g = (+)0.38 \pm 0.04.$$

The experimental uncertainty in this radioactive-beam g-factor measurement is of the order of 10%, which compares favorably with many stable-beam g-factor measurements. It is worth noting that the overall error is due to the uncertainty of $\pm 7.7\%$ in the lifetime, in combination with uncertainties of similar magnitude in the procedure used to fit, and extrapolate, the measured G_k values. Because the g factors adopted for calibration are larger, the magnitude here is somewhat larger than reported previously. Nevertheless, the present result agrees, within errors, with that obtained previously, namely, $|g| = 0.35 \pm 0.05$ [2].

Figure 3 indicates that the experimental g factor of ^{132}Te is consistent with the $g(2^+)$ systematics in the $A \sim 130$ region, and that it has a comparable magnitude to the $g(2_1^+)$ values in the neighboring $N = 80$ isotones of Xe and Ba. This agreement with the systematics gives confidence in the technique. The experimental g factors in ^{130}Te and ^{132}Te are compared with theoretical predictions in Fig. 4. Most of the theories predict a more pronounced increase in the g factor for ^{132}Te, compared with ^{130}Te, than is found experimentally.

IV. RIV—MODELS

A. Static model

In this section an attempt is made to model the vacuum deorientation coefficients for the Te isotopes in terms of a simple static model, along the lines of similar models discussed in Refs. [4,14,15,31]. According to this approach, the observed attenuation coefficients, which may be either time dependent or time integral, are given by

$$G_k = \sum_{i,j} w_J(J_i) w_B(B_j) G_k(J_i, B_j), \tag{14}$$

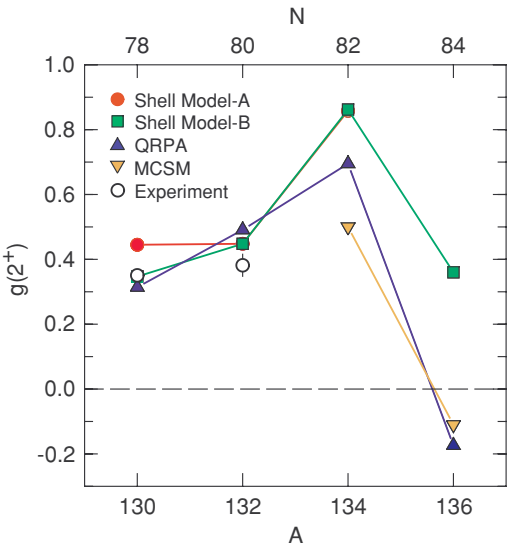

FIG. 4. (Color online) Theoretical g factors in the Te isotopes compared with experiment. Shell model calculations A and B are from [24,28], respectively. QRPA is from [29] and MCSM from [30].

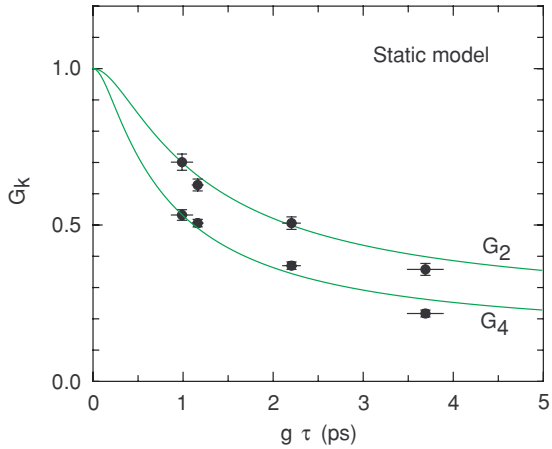

FIG. 5. (Color online) Time integral attenuation coefficients for the Te isotopes compared with the static model discussed in the text.

where the contributing attenuation coefficients, $G_k(J_i, B_j)$, are evaluated from Eqs. (2)–(5). In the present work the weights associated with the atomic spin and the hyperfine field, w_J and w_B, respectively, are assumed to be normalized Gaussian distributions, specified by their mean and standard deviations denoted $\bar{J}$ and σ_J for w_J, and $\bar{B}$ and σ_B for w_B. These distributions, which have $\bar{B} \geqslant 0$ and $\bar{J} \geqslant 0$, are cut off at $J = 0$ and $B = 0$. Clearly $J \geqslant 0$ and J takes only integer or half-integer values. The magnetic field distribution is assumed to be continuous. Because the attenuation coefficients are independent of the sign of B, the calculations can be restricted to $B \geqslant 0$.

The present data prove rather insensitive to the precise shape of the magnetic field distribution (see below). Lorentzian field distributions, as discussed in Sec. II, were not used in the present model because measures of the average hyperfine field at the nucleus such as $\langle |B| \rangle$ and $\langle B^2 \rangle^{1/2}$ are infinite unless a high-field cutoff is introduced. This physically unrealistic feature does not occur when Gaussian distributions are assumed.

1. Te isotopes at $v \sim 0.06c$

An extensive search of the static model parameter space was made for fits to the RIV data on the Te isotopes. It was found that the parameters of the magnetic field distribution, namely the mean, $\bar{B}$, and the width, σ_B, are strongly correlated, which indicates that the data are not very sensitive to the shape of the distribution. Because the fits tend to favor $\sigma_B \approx \bar{B}$ with a shallow chi-squared, the number of parameters was reduced by fixing $\sigma_B = \bar{B}$.

For the atomic spin parameters, the fits tend to favor a narrow distribution, $\sigma_J \sim 1$. If unconstrained, the average spin, $\bar{J}$, tends toward unrealistic values as high as $20\hbar$. However the chi-squared distribution becomes almost flat for $\bar{J} > 4.5$. It is reasonable (and necessary) therefore to fix $\bar{J} = 4.5$, an average spin value that is consistent with the conclusions of previous work: Andrews *et al.* [13] reported $\bar{J} \sim 3.5$ for Cd ions recoiling with $v = 0.01c$, Dafni *et al.* [32] found $\bar{J} = 5(1)$ for Gd and $\bar{J} = 3$ for Fe (both with $v = 0.018c$), and Billowes [23] suggested $\bar{J} > 3$ for W, Os, and Pt ions entering vacuum with $v = 0.02c$.

Figure 5 compares the experimental attenuation factors for the Te isotopes with the static model fit. Here, as in Fig. 2, it is convenient to plot the G_k values as a function of the product $g\tau$, which is an invariant in static models of RIV. The calculation shown in Fig. 5 has $\bar{J} = 4.5$, $\sigma_J = 1$ and $\sigma_B = \bar{B}$. The best fit corresponds to $\bar{B} = 8.8$ kT or $\langle B^2 \rangle^{1/2} = 14.3$ kT. This value for the average hyperfine field seems reasonable for Te ions that recoil into vacuum with a velocity of $v = 0.062c$ and therefore have an average charge state near 30+, with the (atomic) Fermi level in the vicinity of the 3d and 4s orbits.

The magnitude of the average hyperfine field, which should increase with both ion velocity and atomic number, also appears to be consistent with previous work at lower ion velocities. For example, Dafni *et al.* [32] reported an average field of 2.8 kT for Gd at $v = 0.018c$ and Andrews *et al.* [13] used $\bar{B} = 0.35$ kT and $\sigma_B = 0.525$ kT to describe the RIV interaction for Cd at $v = 0.01c$.

2. Nuclear spin dependence of vacuum deorientation

An early study by Ward *et al.* [12] examined the time-integral vacuum deorientation of the 2_1^+ and 4_1^+ states in ^{150}Sm and the 6_1^+ and 8_1^+ states in ^{156}Gd recoiling into vacuum with velocities of $v = 0.029c$. In line with what was known about RIV at the time, Ward *et al.* analyzed their data in terms of the Abragam-Pound theory, which predicts that the RIV interaction is independent of the nuclear spin. They came to the conclusion that $g(4_1^+)$ is significantly higher than $g(2_1^+)$ in ^{150}Sm. Such behavior is difficult to reconcile with theoretical expectations and subsequent transient-field studies [33,34]. In contrast, according to the static model, the G_k parameters have nuclear spin sensitivity through the coupling of $\boldsymbol{I}$ and $\boldsymbol{J}$ to $\boldsymbol{F}$

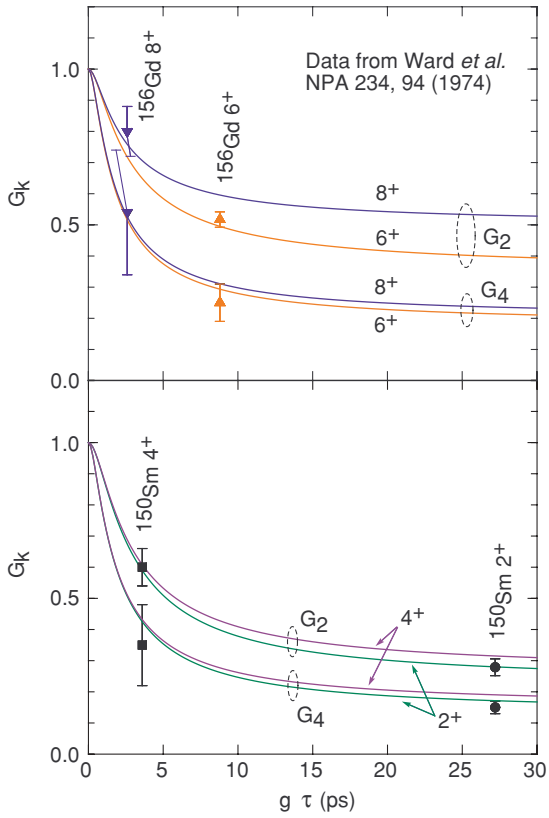

FIG. 6. (Color online) Static model analysis of the attenuation coefficients reported by Ward *et al*. [12] for Sm and Gd ions recoiling in vacuum.

by the factors $C_{IJ}^{FF'}(k)$, Eq. (3). The nuclear spin dependence of the data of Ward *et al*. was therefore reexamined in the present static model.

The experimental G_2 and G_4 values from Table 2 of [12] were reanalyzed. As for the Te isotopes, the atomic spin parameters were fixed at $\bar{J} = 4.5$ and $\sigma_J = 1$. The width of the hyperfine field distribution was also constrained by setting $\sigma_B = \bar{B}$, leaving $\bar{B}$ as the only free parameter. The required g factors were taken from the compilation of $g(2_1^+)$ values in [35], making the assumption that all relevant g factors in the ground bands of ^{150}Sm and ^{158}Gd are the same up to $I = 8$, which is consistent with several transient-field studies [33,34,36]. As shown in Fig. 6, the resultant fit, for $\bar{B} = 3.7(5)$ kT, is in very good agreement with the data. In contrast with the Abragam-Pound fluctuating model analysis, the static model analysis of the data is perfectly consistent with $g(4_1^+) = g(2_1^+)$ in ^{150}Sm. A time-differential study on ^{150}Sm recoiling into vacuum at a velocity of $v = 0.019c$ by Ward *et al*. [11] has also been successfully reanalyzed in terms of a purely static perturbation by Goldring *et al*. [14]. Concerning the atomic spin dependence, the data of Ward *et al*. [12] are clearly consistent with $\bar{J} = 4.5$. Unfortunately the data do not have sufficient precision to place a tight constraint on the atomic spin distribution assumed by the model. Further measurements on nuclear states with spins other than $I = 2$ are required.

B. Static model with fluctuations

The comparisons in Figs. 5 and 6 show a high level of agreement between the static model and experiment. For the more precise data on the Te ions, however, the fit is less than perfect. In particular, the experimental attenuation coefficients for ^{122}Te are smaller than predicted, which suggests that the pure static model considered in the previous section is too simple. The over-estimation of the G_k values at longer times (i.e., for ^{122}Te) implies that the 'hard core' values of the attenuation coefficients must be reduced. This reduction, which could not be achieved with the pure static model and realistic parameters, is most naturally explained by allowing some atomic fluctuations to occur.

An ion entering vacuum in a highly excited state after emerging from a foil can relax through the emission of photons and/or Auger electrons. While such processes are no longer considered to dominate the hyperfine interactions of heavy ions in vacuum over the nuclear lifetime range considered here, atomic transitions must make some contribution to the loss of nuclear orientation.

A model which uses a Monte Carlo approach to allow atomic fluctuations will now be considered. As in the static model described above, the initial spin distribution and the hyperfine field distribution are assumed to be Gaussian. When a transition takes place B is reset at random, within its specified distribution, and J is allowed to change by $\Delta J = 0, \pm 1$, with equal probability.

Two parameters are introduced to control the time evolution of the system: τ_E is the parameter that determines how often the ensemble *tries* to make a fluctuation, whereas τ_A is the parameter that determines whether the atom is *allowed* to make the transition. In the limit that τ_E is small and $\tau_A \to \infty$, the system fluctuates continually. The static limit, identical to the model described in the previous section, occurs when $\tau_A \to 0$. For an intuitive picture, τ_A can be considered the mean time for an average ion to reach its ground state, whereas τ_E can be considered an average lifetime of the excited atomic levels. The number of electronic configuration changes that occur approaches τ_A/τ_E at long times.

This model is very simple but has sufficient flexibility to describe the effect of atomic transitions varying from the limit of continuous rapid fluctuations to the static limit where there are no fluctuations at all. With the aid of the model it can be demonstrated that physical reality is closer to the static limit. The upper panel of Fig. 7 shows the best fit to the attenuation coefficients for three fluctuating scenarios. The lower panel indicates the number of fluctuations as a function of time. For comparison with the static model calculations in Fig. 5, the data are again plotted as a function of $g\tau$. In models with fluctuations $g\tau$ is no longer an invariant. For display purposes, the G_k values have therefore been evaluated for fixed $g = 0.35$ and varying lifetime, which is a valid approximation for the Te isotopes.

For the schematic calculations in Fig. 7, the initial value of J was chosen from a Gaussian distribution with $\bar{J} = 4.5$ and $\sigma_J = 1$. The parameters τ_E and τ_A were chosen to represent particular fluctuating conditions; $\bar{B}$ and σ_B were then adjusted to fit the data. The first case, labeled A in Fig. 7, has $\tau_E = 1/3$ ps and $\tau_A \to \infty$ and comes closest to the Abragam-Pound

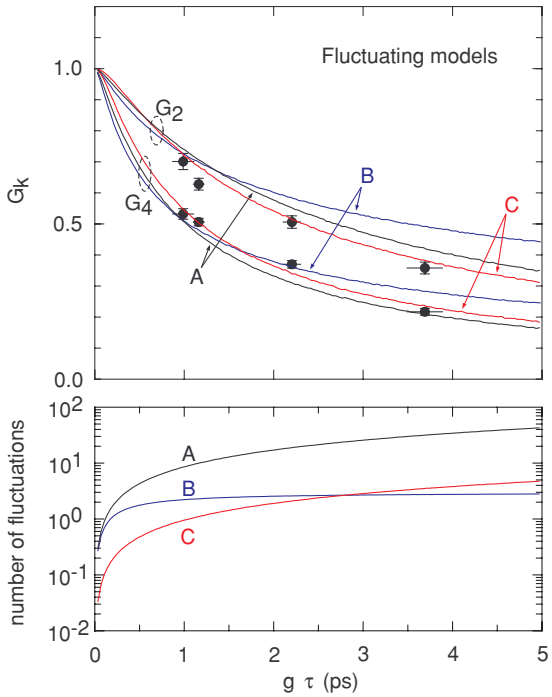

FIG. 7. (Color online) Integral attenuation coefficients for three fluctuating scenarios (upper panel). The $G_k(\infty)$ values have been evaluated for fixed $g = 0.35$ and varying lifetime The lower panel indicates the average number of fluctuations as a function of time. Case A has an average of three fluctuations per picosecond continuously; case B has three fluctuations in the first picosecond; case C has 3 ps between fluctuations.

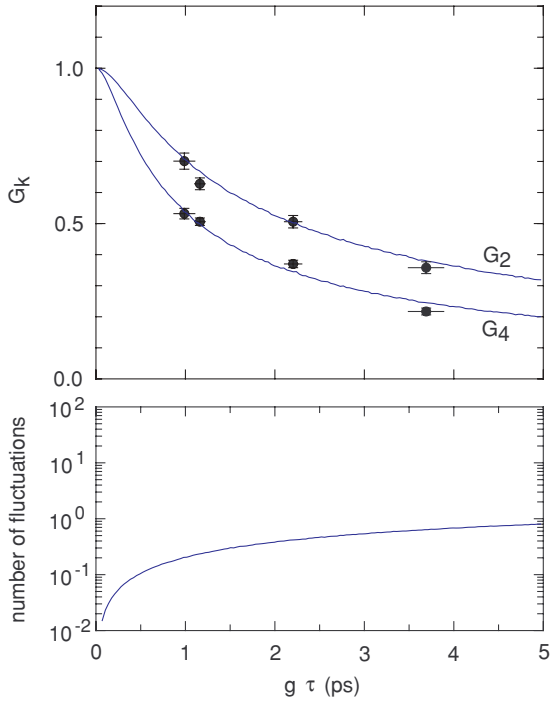

FIG. 8. (Color online) As for Fig. 7, but near the static limit of the Monte Carlo model ($\tau_E = 13$ ps, $\tau_A = 39$ ps). This case represents the 'best' fit achieved with the present model.

limit. Like all models with too many fluctuations, the quality of the fit to the data in case A is rather poor because the ratio G_4/G_2 is too small. The second case (B), with $\tau_E = 1/3$ ps and $\tau_A = 1$ ps, indicates the effect of a few fluctuations within the first picosecond of the ion emerging into vacuum. The description of the data is again worse than for the pure static model, which demonstrates that if there are any rapid atomic transitions immediately after the ion enters vacuum, they are so fast and/or the fields are so weak that the perturbation of the nuclear orientation is very small.

The final example (C), having $\tau_E = 3$ ps and $\tau_A \to \infty$, resembles the fluctuating scenario with correlation time $\tau_c = \tau_E$, that at first seemed applicable to RIV [10]. A much improved description of the data is obtained. This model, however, does not correspond to the Abragam-Pound (AP) fluctuating model [9] that was often used in the early analysis of RIV data. The AP model requires that there be many fluctuations during the nuclear lifetime and that the nuclear precession be small between fluctuations. Neither of these conditions is fulfilled: From the lower panel of Fig. 7 it can be seen that in case C there are on average only four or fewer transitions within the lifetime of the Te 2^+ levels. Furthermore, according to the fitted field parameters, the nuclear precession in 3 ps is rather large, of the order of 0.5 rad.

It can be concluded that for the Te isotopes recoiling into vacuum with $v \sim 0.06c$ there are relatively few fluctuations on a time scale up to 11 ps, the longest mean life in the present study. This conclusion is in good general agreement with previous work. Goldring *et al.* [14] found that the characteristic fluctuation time for Sm ions recoiling into vacuum with $v \sim 0.014c$ is about 150 ps, and Andrews *et al.* concluded that the $21/2^+$ state of ^{107}Cd had reached the static state within 50 ps after emerging into vacuum with $v = 0.01c$.

A more realistic description of the present data requires that τ_A take a finite value. Unfortunately it has proved impossible to determine τ_E and τ_A uniquely from the present data set because the range of nuclear lifetimes is limited ($3 < \tau < 11$ ps). However reasonable fits can be obtained for $10 < \tau_E < 20$ ps and $\tau_A/\tau_E \approx 3$. Figure 8 shows the results of a fit with $\tau_E = 13$ ps and $\tau_A/\tau_E = 3$, $\bar{B} = 6.6$ kT and $\sigma_B = 10.9$ kT.

By including a few fluctuations in the period up to about 10 ps, the description of the data is improved compared with the pure static model. The total chi-squared is improved from $\chi^2 = 20.5$, for the pure static model in Fig. 5, to $\chi^2 = 10$, for the static model with fluctuations in Fig. 8. Of course, there is still room for improvement. One avenue for investigation is suggested by the presence of the fluctuations in the first few tens of picoseconds, which may cause the distribution of hyperfine magnetic fields and atomic spins to evolve on this timescale. As more calibration data on nuclear levels with longer lifetimes and higher spins are accumulated it should prove possible to refine the model.

V. IMPLICATIONS FOR *g* FACTOR MEASUREMENTS

As discussed in Sec. III and shown in Fig. 2, the g factor of the 2_1^+ state in ^{132}Te was extracted from an extrapolation of

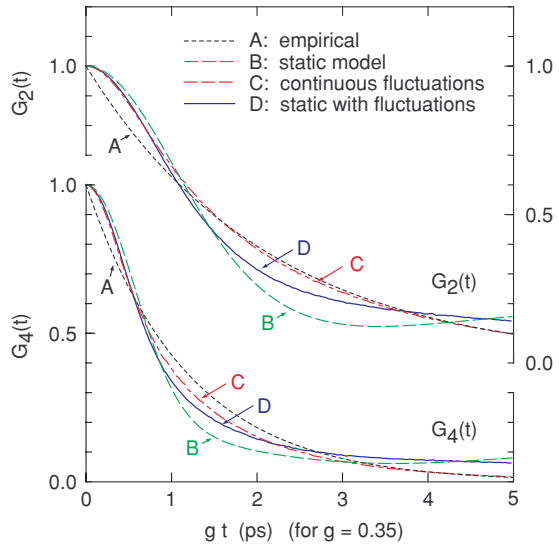

FIG. 9. (Color online) Comparison of time differential attenuation coefficients. For comparisons with the previous figures, the horizontal axis shows the product $g \times t$ with $g = 0.35$ fixed. Case A corresponds to the empirical (Lorentzian model) fit used to extract $g(2_1^+)$ in ^{132}Te (Fig. 2). Case B corresponds to the best pure static model fit (Fig. 5). Case C corresponds to case C Fig. 7 (i.e., continuous fluctuations with 3 ps between fluctuations on average). Case D corresponds to the 'best' model-based fit shown in Fig. 8.

calibration data for ^{122}Te, ^{126}Te, and ^{130}Te, based on Eq. (10) with Γ_k and α_k treated as free parameters. It is apparent from the comparisons with the model-based calculations shown in Figs. 5, 7 (case C), and 8, that several of the model-based fits reproduce the experimental G_k values and the extracted g factor for ^{132}Te very well. The implication is that any of these models could have been used for the extrapolation and would have yielded the same g factor for ^{132}Te, well within the assigned experimental uncertainties.

Figure 9 compares the time differential attenuation coefficients for the three best model fits with those that correspond to the empirical fit used to extract $g(2^+)$ in ^{132}Te. Although the time dependent attenuation factors $G_k(t)$ differ from model to model, and are not exactly exponential as assumed for the g-factor analysis, the time-integral attenuation factors $G_k(\infty)$ tend to average out the differences. It is evident that uncertainties in modeling the vacuum attenuation are mitigated, and that the integral attenuation coefficients can be quite insensitive to details of the time-dependent factors. Furthermore, in the present case, uncertainties are reduced by the fact that the lifetime and the g factor in the calibration nucleus ^{130}Te are similar in magnitude to those in ^{132}Te.

These considerations demonstrate that the use of the empirical approach to extract the experimental g factor in ^{132}Te was justified. Looking to a future measurement on ^{134}Te, which has $\tau = 1.2$ ps [21], it is reassuring to see that the three different models shown in Fig. 9 have rather similar $G_k(t)$ values at short times, i.e., for $t \lesssim 3$ ps (or $gt \lesssim 1$ ps). For ^{136}Te, however, which has a considerably longer lifetime ($\tau \sim 50$ ps [21]), the extrapolation of the calibration data available at present is less clear-cut. On one hand, most of the deorientation takes place in the first 10 ps where the interaction is well calibrated. But on the other hand, the magnitude of the 'hard core' terms at longer times depends sensitively on the number and distribution in time of a few atomic fluctuations, which is not well determined. A careful model-based analysis will be required, supplemented by additional calibration data. For example, the $3/2_2^+$ and $5/2_1^+$ states in ^{125}Te, having mean lives of 28 ps and 19 ps, respectively [37], provide a means to probe the RIV interaction at longer times than is possible with the even isotopes.

A purely empirical calibration may prove sufficient for the ^{136}Te case, however from the perspective of modeling RIV the important directions for future development are (i) to more stringently constrain the timescales associated with the atomic fluctuations—especially when they cease, and (ii) to evaluate the extent to which the atomic parameters such as $\bar{B}$, σ_B, $\bar{J}$, and σ_J, evolve in time.

VI. SUMMARY AND CONCLUDING REMARKS

In the light of the new g factor results for ^{126}Te and ^{130}Te [1], the radioactive beam g-factor measurement on ^{132}Te was reevaluated. The resultant g factor agrees, within errors, with the earlier analysis. A description of the semiempirical procedure used to extract the g factor from the experimental deorientation coefficients was given, and its theoretical basis was discussed.

Models of the RIV interaction together with fits to the experimental data [2] show that for Te ions with $v \sim 0.06c$, the interaction is predominantly static with a superposition of many hyperfine frequencies. This conclusion is consistent with previous work on slower moving ions. To explain the data, however, there are very strong indications that a few ($\lesssim$4) atomic transitions occur in the time up to about 10 ps. Future investigations must evaluate the extent to which the distribution of hyperfine fields and atomic spins evolves on this time scale and define the consequences for g-factor measurements. Experimentally, it is particularly important to characterize the interaction at times beyond 10 ps. Further experiments are also needed to calibrate the velocity and atomic spin dependence of the RIV interaction in the region near ^{132}Sn, for future applications to radioactive beam g-factor measurements.

ACKNOWLEDGMENTS

This work, funded in part by U.S. DOE Grant No. DE-FG02-96ER40983, was motivated by the radioactive beam g-factor measurement in Refs. [2,17,18] and collaboration with those authors. A.E.S. acknowledges travel support from the Joint Institute for Heavy Ion Research, Oak Ridge National Laboratory. Very useful discussions with Jim Beene concerning the modeling of the RIV interaction are gratefully acknowledged. Carrol Bingham and Cyrus Baktash are thanked for their encouragement and support.

[1] A. E. Stuchbery, A. Nakamura, A. N. Wilson, P. M. Davidson, H. Watanabe, and A. I. Levon, Phys. Rev. C **76**, 034306 (2007).
[2] N. J. Stone, A. E. Stuchbery, M. Danchev, J. Pavan, C. L. Timlin, C. Baktash, C. Barton, J. Beene, N. Benczer-Koller, C. R. Bingham *et al*., Phys. Rev. Lett. **94**, 192501 (2005).
[3] G. Goldring, in *Heavy Ion Collisions*, edited by R. Bock (North-Holland, Amsterdam, 1982), Vol. 3, p. 484.
[4] G. Goldring and H. Hass, in *Magnetic Moments of Short-Lived Levels*, Vol. 3 of *Treatise on Heavy-Ion Science*, edited by D. A. Bromley (Plenum Press, New York, 1985), p. 539.
[5] G. Goldring, D. A. Hutcheon, W. L. Randolph, D. H. F. Start, M. B. Goldberg, and M. Popp, Phys. Rev. Lett. **28**, 763 (1972).
[6] A. E. Stuchbery, P. F. Mantica, and A. N. Wilson, Phys. Rev. C **71**, 047302 (2005).
[7] A. E. Stuchbery and M. P. Robinson, Nucl. Instrum. Methods Phys. Res. A **485**, 753 (2002).
[8] K. Alder and A. Winther, *Electromagnetic Excitation* (North-Holland, Amsterdam, 1975).
[9] A. Abragam and R. V. Pound, Phys. Rev. **92**, 943 (1953).
[10] I. Ben Zvi, P. Gilad, M. Goldberg, G. Goldring, A. Schwarzschild, A. Sprinzak, and Z. Vager, Nucl. Phys. **A121**, 592 (1968).
[11] D. Ward, R. L. Graham, J. S. A. H. R. Geiger, and N. Rud, Nucl. Phys. **A193**, 479 (1972).
[12] D. Ward, A. H. R., R. L. Graham, J. S. Geiger, and N. Rud, Nucl. Phys. **A234**, 94 (1974).
[13] H. R. Andrews, R. L. Graham, J. S. Geiger, J. R. Beene, O. Häusser, D. Ward, and D. Horn, Hyperfine Interact. **4**, 110 (1978).
[14] G. Goldring, K. Hagemeyer, N. Benczer-Koller, R. Levy, Y. Lipshitz, B. Richter, Z. Shkedi, Y. Wolfson, and K. H. Speidel, Hyperfine Interact. **5**, 283 (1978).
[15] R. Brenn, H. Spehl, A. Weckherlin, H. A. Doubt, and G. van Middelkoop, Z. Phys. A **281**, 219 (1977).
[16] Y. Niv, M. Hass, and A. Zemel, Hyperfine Interact. **8**, 19 (1980).
[17] N. J. Stone, A. E. Stuchbery, M. Danchev, J. Pavan, C. L. Timlin, C. Baktash, C. Barton, J. Beene, N. Benczer-Koller, C. R. Bingham *et al*., Eur. Phys. J. A Direct **25**, s01, 205 (2005).
[18] M. Danchev, J. Pavan, N. J. Stone, A. E. Stuchbery, C. Baktash, J. Beene, N. Benczer-Koller, C. R. Bingham, J. Dupak, A. Galindo-Uribarri *et al*., Nucl. Instrum. Methods Phys. Res. B **241**, 971 (2005).
[19] A. E. Stuchbery and P. F. Mantica, Proceedings of RNB7 (to be published in Eur. Phys. J. A Direct).
[20] S. Raman, C. W. Nestor, and P. Tikkanen, At. Data Nucl. Data Tables **78**, 1 (2001).
[21] D. C. Radford, C. Baktash, J. R. Beene, B. Fuentes, A. Galindo-Uribarri, C. J. Gross, P. A. Hausladen, T. A. Lewis, P. E. Mueller, E. Padilla *et al*., Phys. Rev. Lett. **88**, 222501 (2002).
[22] C. J. Barton, M. A. Caprio, D. Shapira, N. V. Zamfir, D. S. Brenner, R. L. Gill, T. A. Lewis, J. R. Cooper, R. F. Casten, C. W. Beausang *et al*., Phys. Lett. **B551**, 269 (2003).
[23] J. Billowes, Hyperfine Interact. **30**, 265 (1986).
[24] G. Jakob, N. Benczer-Koller, G. Kumbartzki, J. Holden, T. J. Mertzimekis, K. H. Speidel, R. Ernst, A. E. Stuchbery, A. Pakou, P. Maier-Komor *et al*., Phys. Rev. C **65**, 024316 (2002).
[25] J. M. Brennan, M. Hass, N. K. B. Shu, and N. Benczer-Koller, Phys. Rev. C **21**, 574 (1980).
[26] N. J. Stone, At. Data Nucl. Data Tables **90**, 75 (2005).
[27] M. Sambataro and A. E. L. Dieperink, Phys. Lett. **B107**, 249 (1981).
[28] B. A. Brown, N. J. Stone, J. R. Stone, I. S. Towner, and M. Hjorth-Jensen, Phys. Rev. C **71**, 044317 (2005).
[29] J. Terasaki, J. Engel, W. Nazarewicz, and M. Stoitsov, Phys. Rev. C **66**, 054313 (2002).
[30] N. Shimizu, T. Otsuka, T. Mizusaki, and M. Honma, Phys. Rev. C **70**, 054313 (2004).
[31] C. L. Timlin, Project Report, Oxford University (2004) (unpublished).
[32] E. Dafni, J. Bendahan, C. Broude, G. Goldring, M. Hass, E. Naim, M. H. Rafailovich, C. Chasman, O. C. Kistner, and S. Vajda, Nucl. Phys. **A443**, 135 (1985).
[33] A. P. Byrne, A. E. Stuchbery, H. H. Bolotin, C. E. Doran, and G. J. Lampard, Nucl. Phys. **A466**, 419 (1987).
[34] F. Brandolini, in *Perspectives for the Interacting Boson Model*, edited by R. F. Casten *et al*. (World Scientific, Singapore, 1994), p. 647.
[35] A. E. Stuchbery, Nucl. Phys. **A589**, 222 (1995).
[36] A. E. Stuchbery, A. G. White, G. D. Dracoulis, K. J. Schiffer, and B. Fabricius, Z. Phys. A **338**, 135 (1991).
[37] J. Katakura, Nuclear Data Sheets **86**, 955 (1999).